Structural Model of a Cyclic Dynorphin A Analog Bound to Dodecylphosphocholine Micelles by NMR and Restrained Molecular Dynamics

Michael R. Tessmer,† Jean-Philippe Meyer,‡ Victor J. Hruby,‡ and Deborah A. Kallick*,†

Department of Medicinal Chemistry, College of Pharmacy, University of Minnesota, 308 Harvard Street SE, Minneapolis, Minnesota, 55455, and Department of Chemistry, University of Arizona, Tucson, Arizona 85721

Received July 30, 1996⊗

The compound c[Cys^{5,11}]dynorphin A-(1−11)-NH_2, **1**, is a cyclic dynorphin A analog that shows similar selectivity and potency at the κ-opioid receptor when compared to the native form of the peptide in central nervous system assays. Previous molecular mechanics calculations have shown that the ring portion of the isoform that is *trans* about the Arg^9−Pro^{10} ω bond contains either a β-turn from residues Arg^6 to Arg^9 or an α-helical conformation. Our results from solution state NMR indicate that the compound exhibits *cis*−*trans* isomerism about the Arg^9−Pro^{10} ω bond in both aqueous solution and when bound to dodecylphosphocholine micelles. Restrained molecular dynamics calculations show that the *cis* isoform of the peptide contains a type III β-turn from residues Arg^7 to Pro^{10}. Similar calculations on the *trans* isoform show it to contain a β-turn from residues Cys^5 and Arg^8. In this report we describe the generation of three-dimensional models from NMR data for the ring portions of both the *cis* and *trans* isoforms of **1** bound to dodecylphosphocholine micelles. Comparison with other dynorphin A structural information indicates that both the *cis* and *trans* isoforms of the peptide may be active as κ-opioid agonists.

Introduction

Presented in this report are three-dimensional models of the *cis* and *trans* isoforms about the Arg^9−Pro^{10} ω peptide bond of a cyclic dynorphin analog bound to dodecylphosphocholine (DPC) micelles as studied by solution NMR and restrained molecular dynamics. The cyclized dynorphin analog c[Cys^{5,11}]-Tyr-Gly-Gly-Phe-Cys-Arg-Arg-Ile-Arg-Pro-Cys-dynorphin A-(1−11)-NH_2 (**1**) was made by substituting L-cysteines for residues Leu^5 and Lys^{11} of the native dynorphin-(1−11) sequence to create a 23-membered disulfide-linked ring.[1] Analog **1** has been shown to have a binding affinity and selectivity profile for the κ-opioid receptor similar to that of the native form of the peptide in central nervous system assays.[2] The analog retains κ-opioid selectivity in guinea pig brain homogenates and displays a large preference for κ-opioid receptors in the brain over those in the periphery.[1,2] The different activity patterns in the central vs peripheral assays indicates the possible existence of subtypes of κ-opioid receptors located in different tissues.[2]

Structure−activity studies on opioid peptides have concentrated on the δ and μ receptors so that less is known about the specific binding requirements at the κ-opioid receptor. As an example of the lack of structure−activity studies, the specific residues of dynorphin which cause its κ-selectivity are still in question. It was initially thought that the basic residues of Arg^6, Arg^7, and Lys^{11} were the key determinants in κ-opioid selectivity; however, the importance of these residues in dynorphin has not been entirely reproducible.[3−5] Studies on **1** as well as other analogs of dynorphin will be one of the key ways in determining the exact binding requirements for κ-opioid selectivity. Further development of selective ligands is important for determining the specific conformational and topographical requirements that dictate interactions between κ-opioid ligands and their receptors. This study also has the advantage of examining a ligand that is both bound to a lipid micelle and cyclized. These are both techniques that have been shown to reduce the inherent conformational flexibility in peptides, thereby making solution NMR studies more feasible.[6−9] In addition to stabilizing peptide secondary structure, DPC micelles also serve to mimic the peptide−lipid interactions that have been shown to be potentially important for biological activity.[10−12]

Recent molecular mechanics studies on **1** have shown that two distinct conformations, both of which are *trans* about the Arg^9−Pro^{10} ω bond, may be present.[13] These two conformations were proposed to be the binding conformations of dynorphin at central κ-opioid receptors. The two major conformations of the molecule found were a β-turn centered around residues Arg^7 and Ile^8 and an α-helical region starting at Gly^3 and extending into the ring. Previous results from our laboratory on the full-length dynorphin have shown the molecule to be α-helical from residues Gly^3 to Pro^{10} and to contain a β-turn at the C-terminus.[14,15] We report here two major conformations for **1** in slow exchange on the NMR chemical shift time scale due to *cis*−*trans* isomerism around the Arg^9−Pro^{10} ω bond. To our knowledge, this is the first time that *cis*−*trans* isomerism has been seen at the Arg^9−Pro^{10} ω bond in the native dynorphin or any of its analogs. Refinement of the initial distance geometry generated structures via restrained molecular dynamics (rMD) shows that the *cis* isoform of the peptide contains a type III β-turn between residues Arg^7 and Pro^{10}. The same calculations on the *trans* isoform of the peptide indicate that its predominant form is that of a β-turn centered around residues Arg^6 and Arg^7. This report details the generation of the three-dimensional models of the *cis* and *trans* isoforms of **1** as well as

* To whom correspondence should be addressed.
† University of Minnesota.
‡ University of Arizona.
⊗ Abstract published in *Advance ACS Abstracts,* June 15, 1997.

S0022-2623(96)00562-6 CCC: $14.00

relating the information to earlier models from other dynorphin studies.

Materials and Methods

Sample Preparation. The dynorphin A-(1−11) analog c[Cys^{5,11}]-Tyr-Gly-Gly-Phe-Cys-Arg-Arg-Ile-Arg-Pro-Cys-dynorphin A-(1−11)-NH_2 (**1**) was synthesized and purified as reported previously.[1] Dodecylphosphocholine-d_{38} (DPC) was obtained from MSD Isotopes (Montreal, Canada), 99.9% D_2O from Cambridge Isotope Labs (Cambridge, MA), 99.9% D_2O with 0.75% 2,2,3,3-tetradeuterio-3-(trimethylsilanyl)propionic acid (TSP) from MSD Isotopes, and sodium phosphate from Baker Analytical Reagents (Phillipsburg, NJ). The DPC bound sample of **1** used for NMR data collection was 8.03 mM in **1**, 83.4 mM DPC-d_{38}, and 10 mM PO_4^{3-} at pH 3.4 in 90% H_2O/10% D_2O. The sample of **1** for experiments without DPC present was 2.18 mM in **1** with 10 mM PO_4^{3-} at pH 3.4 in 90% H_2O/10% D_2O as well as in 100% D_2O. TSP was used as the internal chemical shift standard.

NMR Experiments. All NMR experiments were performed on either a Bruker AMX-500 or AMX-600 spectrometer and analyzed on a Silicon Graphics Personal Iris with FELIX v2.30 (Biosym, San Diego). Total correlation spectroscopy (TOCSY) and nuclear Overhauser spectroscopy (NOESY) experiments, performed as described below, were used to assign the ^{1}H resonances with the standard sequential assignment method.[16] Presaturation of the solvent peak during the relaxation delay (as well as the mixing time in NOESY and ROESY spectra) was performed for suppression of the solvent resonance in all spectra. Spectra used for analysis were collected at 288 K, as it was determined that spectral overlap was at a minimum at that temperature.

TOCSY experiments with mixing times of 50 and 75 ms were obtained at 600 MHz with a spectral width of 7812.500 Hz in both dimensions using TPPI phase cycling.[17] In a typical experiment, 512 equally spaced t_1 increments were acquired with 64 scans of 2048 complex points per t_1 value and 16 dummy scans prior to data acquisition to equilibrate the sample. Apodization in the t_2 dimension was done with a squared sine bell function (512 points, 90° phase) and in the t_1 dimension with a squared sine bell function (512 points, 90° phase) as well. The data was then zero filled to yield a 2K × 2K real matrix.

The standard NOESY pulse sequence of Macura and Ernst[18] was utilized for ^{1}H assignment and for the determination of distance restraints. The spectra were obtained at 500 MHz with a spectral width of 6024.096 Hz in both dimensions and TPPI phase cycling.[17] A normal experiment consisted of 400 t_1 increments with 48 scans of 2048 complex points per t_1 value. In the t_2 dimension, apodization was done with a skewed sine bell squared function (400 points, 90° phase, and 0.9 skew). In the t_1 dimension, linear prediction of one-third more experiments[19] was followed by the application of a skewed sine bell squared function (540 points, 90° phase, and 0.9 skew) and zero filling to yield a 2K × 2K real matrix. All NOESY data sets were baseline corrected in both dimensions using a polynomial function prior to spectral analysis. ROESY spectra on **1** with and without DPC present were collected at 500 MHz with a mixing time of 65 ms in each case.[20,21] Spectral widths were 6024.096 Hz in both dimensions, and each experiment consisted of 48 scans by 400 t_1 increments. The phase cycling, apodization, linear prediction, zero filling, and baseline correction were the same as those used for the NOESYs.

Structural Determination and Computational Modeling. Interproton distances for all NOESY cross peaks in a 175 ms mixing time spectrum were assigned an upper distance limit of 5.0 Å and a lower limit of 1.8 Å. The lower limit represents the sum of the van der Waals radii of the interacting atoms and the upper limit the standard NOE cutoff distance. Distances were not classified into the standard categories of strong, medium, and weak since many of the peptide resonances were identical in the *cis* and *trans* isoforms (see chemical shift data in Table 2).[22]

Initial structure generation from random coordinates with the DIANA algorithm was used as the first step in determining the three-dimensional models of the *cis* and *trans* isoforms of analog **1** bound to DPC micelles.[23,24] DIANA uses the distance restraint information obtained from the NOESY experiments outlined above as input for the calculations. The distance restraint lists contained 114 and 97 atom pairs for the *cis* and *trans* isoforms, respectively. Due to degeneracy in the 2,6 and 3,5 aromatic protons of tyrosine and phenylalanine, and the lack of stereospecific assignments for the diastereomeric protons, pseudoatom modifications to the input data were made in certain cases.[16] The presence of the disulfide bond from Cys^5 to Cys^{11} was declared in the DIANA sequence file and fixed with distance constraints in the form of upper and lower distance limits.[25] Specifically, the S−S distance was fixed to a range between 2.0 and 2.1 Å, and the S−C_β interresidue distance was fixed between 3.0 and 3.1 Å. Addition of long-range restraints, and increasing the strength of the van der Waals term, was performed after short-term restraints were first examined by DIANA.[23,24] The effect of this is that the algorithm calculates the local structure before the global structure. Analysis of the 100 DIANA-generated structures for the *cis* and *trans* isoforms showed that the majority fell into a structural class that was unique to each isoform. Similar results were generated with different random seed numbers. Table 1 contains data on the target function values, constraint violations, and van der Waals violations of the 20 DIANA-generated structures with the lowest target function scores.

The 20 structures for both the *cis* and *trans* isoforms with the lowest target function scores from the DIANA-generated data sets were chosen for further analysis with energy minimization and restrained molecular dynamics (rMD) calculations. Steepest descents minimizations with 10 (kcal/mol)/Å^2 flatwell distance restraints were performed on all structures with the Discover 2.9 algorithm (Biosym, San Diego) utilizing the AMBER force field.[26] Minimization proceeded until the change in energy was less than 0.001 kcal/Å. Constant temperature (300 K) rMD simulations were performed following minimization for 200 picoseconds (ps) with 10 (kcal/mol)/Å^2 flatwell distance restraints. For the 20 *cis* isoforms of the peptide studied, the Arg^9−Pro^{10} ω bond was fixed in the *cis* position by applying a 50 kcal/rad^2 force constant. All other ω bonds were fixed in the *trans* position with the application of a 50 kcal/rad^2 force constant. All structures were equilibrated during the first 60 ps of the simulations and then averaged over the final 140 ps for the structural analyses performed with InsightII (Biosym, San Diego). A distance dependent dielectric of $\epsilon = r$ was utilized to implicitly simulate water in all minimizations and rMD runs. An infinite distance was used for determining the nonbonded atom list in order to include all potentially significant interactions.

Results and Discussion

Analog 1 Chemical Shifts. The ^{1}H chemical shifts for the *cis* and *trans* isoforms of **1** bound to DPC micelles at 288 K are presented in Table 2. As can be seen from Table 2, several chemical shifts are redundant in the two isoforms. Among these shifts are those of the first two residues of the peptide (Tyr^1 and Gly^2) and the Gly^3 amide proton, as well as the Arg^7, Ile^8, Arg^9, and Cys^{11} residues. The major chemical shift differences between the *cis* and *trans* isoforms are in the Phe^4, Cys^5, Arg^6, and Pro^{10} residues. The amide resonances from Phe^4, Cys^5, and Arg^6 in the *trans* isoform are 0.15, 0.24, and 0.53 ppm upfield of the equivalent *cis* isoform resonances. For the α-^{1}H resonances, the *trans* Phe^4, Cys^5, and Arg^6 resonances are 0.11, 0.32, and 0.11 ppm downfield of the equivalent *cis* resonances, and the *trans* Pro^{10} α-^{1}H resonance is 0.21 ppm upfield from the equivalent *cis* isoform resonance. These variations in chemical shift are indicative of substantial differences in chemical environment for the residues in question. The degenerate shifts of the Arg^7, Ile^8, Arg^9, and Cys^{11}

Table 1. Structural Statistics for the 20 *Cis* and 20 *Trans* Isoforms of DPC Bound **1**

parameter	*cis* DIANA	*cis* rEM	*cis* rMD	*trans* DIANA	*trans* rEM	*trans* rMD
target function (Å^2)[a]	0.77 ± 0.45			0.21 ± 0.11		
upper limit violations[a]						
number > 0.2 Å	1.40 ± 2.26			0.05 ± 0.22		
sum of violations (Å)	1.09 ± 0.69			0.43 ± 0.22		
maximum violation (Å)	0.21 ± 0.11			0.11 ± 0.04		
lower limit violations[a]						
number > 0.2 Å	0.00 ± 0.00			0.00 ± 0.00		
sum of violations (Å)	0.04 ± 0.06			0.02 ± 0.04		
maximum violation (Å)	0.04 ± 0.04			0.03 ± 0.03		
van der Waals violations[a]						
number	7.20 ± 2.77			2.30 ± 2.13		
sum of violations (Å)	4.38 ± 1.78			2.14 ± 0.82		
maximum violation (Å)	0.62 ± 0.04			0.27 ± 0.08		
average pairwise rmsd[b]						
backbone residues 5−11	0.59 ± 0.34	0.70 ± 0.33	0.85 ± 0.37	0.90 ± 0.40	0.66 ± 0.30	0.95 ± 0.29
heavy atom 5−11	1.95 ± 0.45	2.16 ± 0.54	2.19 ± 0.56	2.22 ± 0.57	2.16 ± 0.38	2.54 ± 0.45
E_{bond}[c]	16.9 ± 1.5	8.8 ± 0.5	8.3 ± 0.5	16.7 ± 0.6	9.1 ± 0.5	9.1 ± 0.6
E_{theta}	27.4 ± 3.1	31.5 ± 5.0	32.1 ± 3.5	27.8 ± 1.8	30.8 ± 3.5	36.9 ± 4.5
E_{phi}	43.2 ± 4.9	21.9 ± 2.9	20.3 ± 2.2	41.2 ± 3.6	19.0 ± 3.1	19.6 ± 2.9
$E_{out-of-plane}$[d]	15.5[b]	0.8 ± 0.4	0.9 ± 0.4	15.5[b]	0.9 ± 0.2	1.0 ± 0.3
E_{H-bond}	−0.8 ± 0.9	−2.9 ± 0.8	−4.4 ± 0.9	−1.0 ± 0.7	−3.1 ± 0.7	−4.8 ± 0.9
E_{VDW}	311.8 ± 104.5	4.5 ± 3.1	−1.1 ± 4.0	216.5 ± 104.0	0.6 ± 3.7	−3.2 ± 3.2
$E_{repulsion}$	582.8 ± 116.5	221.0 ± 9.4	223.4 ± 7.9	490.0 ± 123.1	212.9 ± 8.8	227.2 ± 8.3
$E_{dispersion}$	−271.0 ± 32.2	−216.5 ± 9.7	−224.5 ± 7.7	−273.5 ± 27.3	−221.3 ± 11.8	−230.4 ± 8.1
$E_{coulomb}$	31.3 ± 14.2	−34.6 ± 12.6	−56.6 ± 7.6	28.9 ± 12.1	−32.9 ± 11.8	−67.0 ± 13.0
E_{total}	445.3 ± 104.2	30.0 ± 13.1	−0.5 ± 8.2	345.6 ± 105.6	24.4 ± 10.9	−8.4 ± 7.3
E_{force}[d]	75.8 ± 20.6	16.6 ± 4.8	9.6 ± 2.9	45.8 ± 14.3	16.5 ± 5.8	16.4 ± 7.3
$E_{total+force}$	521.1 ± 105.7	46.6 ± 15.7	9.1 ± 4.7	391.4 ± 108.0	40.9 ± 14.1	8.0 ± 10.5

[a] After DIANA calculations. [b] Average pairwise root mean square deviation in angstroms ± the standard deviation are reported for each family of 20 structures obtained after each step in the calculations, i.e., after DIANA, energy minimization, and restrained MD. All rmsds are reported for the peptide backbone from residues 5−11. [c] Average energies in kcal/mol ± the standard deviation are reported for each family of 20 structures obtained after each step in the calculations as indicated. [d] Out-of-plane value automatically assigned by discover algorithm for DIANA-generated structures. [e] E_{force} represents total value of forcing from distance and dihedral restraints.

Table 2. ^{1}H Resonance Assignments for Micelle-Bound **1** at 288 K[a]

residue	NH	αCH	βH′, βH″	others
Tyr[1]		4.24	3.11, 3.11	2,6H 7.11, 3,5H 6.83
Gly[2]	8.89	3.87, 3.87		
Gly[3]	8.04	3.86, 3.81		
		(3.88, 3.82)		
Phe[4]	8.26	4.59	3.24, 3.03	2,6H 7.22, 3,5H 7.14, 4H[b]
	(8.41)	(4.48)	(3.10, 3.10)	(2,6H 7.27, 3,5H,[b] 4H[b])
Cys[5]	8.37	4.73	3.21, 3.09	
	(8.61)	(4.41)	(3.24, 3.03)	
Arg[6]	8.01	4.24	1.91, 1.79	γH_2 1.60, 1.54, δH_2 3.17, 3.17 ϵNH 7.37
	(8.54)	(4.13)	(1.88, 1.82)	(γH_2 1.64, 1.64, δH_2 3.20, 3.20 ϵNH 7.53)
Arg[7]	8.08	4.27	1.91, 1.80	γH_2 1.60, 1.60, δH_2 3.19, 3.19 ϵNH 7.40
Ile[8]	7.89	4.01	1.98	γH_2 1.48, 1.17, γH_3 0.88 δH_3 0.84
Arg[9]	8.22	4.40	1.99, 1.92	γH_2 1.60, 1.60, δH_2 3.14, 3.14 ϵNH 7.37
Pro[10]		4.41	2.30, 1.97	γH_2 1.97, 1.86, δH_2 3.71, 3.61
		(4.62)	(2.33, 2.15)	(γH_2 1.92, 1.82, δH_2 3.54, 3.48)
Cys[11]	8.76	4.62	3.30, 3.04	
NH_2 cap				7.59, 7.25

[a] Resonances in parentheses are for the *cis* form where the chemical shift differed from the *trans* form [b] Peaks not observed.

residues are either due to the residues being in similar chemical environments in both isoforms or conformational averaging due to rapid motion in those portions of the ring.

Table 3 (Supporting Information) contains the ^{1}H chemical shifts for the peptide at 288 K in H_2O with no DPC present. Upon addition of lipid, the G2 amide shifts downfield by 0.24 ppm and the G3 amide stays nearly constant (0.03 ppm downfield shift), while the F4 (*cis* isoform) and C5 (*trans* isoform) amides move upfield by 0.12 and 0.47 ppm, respectively. These chemical shift changes are consistent with those seen upon DPC titrations with other opioid peptides.[9,27] The Cys[11] amide also shifts downfield by 0.26 ppm upon lipid titration. Surprisingly the *cis* and *trans* ^{1}H resonances of Ile[8] and Arg[9] can be differentiated in aqueous solution, but are degenerate when the peptide is bound to DPC. The major changes in the Pro[10] ^{1}H resonances are in the side chain methylenes of the *trans* isoform, with shift changes generally in the 0.10 ppm range both upfield and downfield upon DPC titration. The Arg[6] and Arg[7] spin systems could not be unambiguously assigned in aqueous solution, therefore, no conclusions could be drawn from the DPC titration concerning those residues. The line widths of the peptide broaden by a factor of approximately 2.0, and the equivalent NOESY experiments on **1** without DPC present shows the absence of most cross peaks (data not shown). These factors indicate an increase in the overall correlation time, τ_c, for **1** when DPC is added to the solution; this

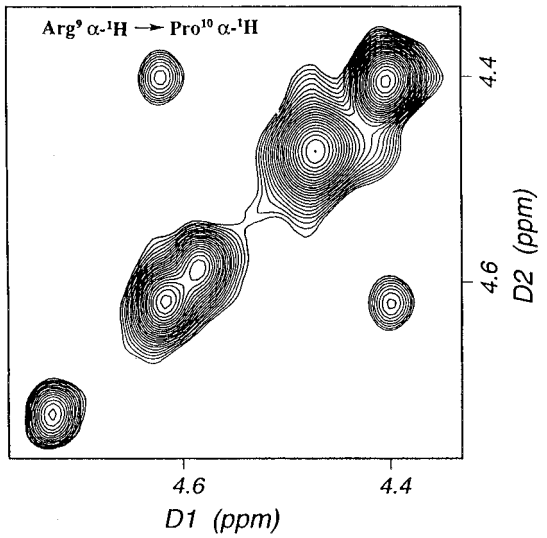

Figure 1. Expansion of a NOESY spectrum at 500 MHz of **1** bound to DPC micelles showing the Arg^9 α-^{1}H to Pro^{10} α-^{1}H cross peak. The spectrum was recorded at 288 K with a mixing time of 125 ms. The sample was 8.03 mM in **1**, 83.4 mM DPC, and 10 mM PO_4^{3-} at pH 3.4 in 90%H_2O/10%D_2O.

is indicative of the peptide binding to the lipid micelle. The lipid to peptide ratio was approximately 10:1 for all 1D and 2D experiments.

Cis−Trans Isomerism. As noted, the peptide exhibits *cis−trans* isomerism around the Arg^9−Pro^{10} ω bond in aqueous solution with no DPC present as well as when bound to DPC micelles. Figure 1 contains a portion of a NOESY spectrum of **1** bound to DPC micelles showing the Arg^9 α-^{1}H to Pro^{10} α-^{1}H cross peak indicative of a *cis* ω bond. No *cis* was observed in the linear dynorphin bound to DPC micelles.[14,15] The *trans* NOEs cannot be unambiguously identified because of chemical shift overlap. In particular, the *trans* Pro^{10} α proton is identical in chemical shift to both the *cis* and *trans* Arg^9 α proton chemical shift. However, both the *cis* and *trans* isoforms can be positively identified in a NOESY spectrum of **1** with no DPC present. Figure 2 contains two portions of a NOESY spectrum of **1** in D_2O with no DPC present that show the Arg^9 α-^{1}H to Pro^{10} δ' and δ'' cross peaks indicative of a *trans* configuration about the Arg^9−Pro^{10} ω bond, and the Arg^9 α-^{1}H to Pro^{10} α-^{1}H cross peak indicative of a *cis* ω bond. The Arg^9 α-^{1}H and Pro^{10} α-^{1}H resonances do not have the same chemical shift when **1** is not bound to DPC, so both isoforms can be shown to exist by the standard diagnostic measures.[16] Since the *cis* isoform can be shown as the minor component in the DPC bound **1** we can infer that the major conformer is the *trans* isoform in the spectrum of DPC bound **1**.

Comparison of the δ' and δ' proline peaks in a 1D spectrum of **1** in the presence of DPC gave a ratio of 2.30:1 at 288 K in favor of the *trans* isoform. This equilibrium ratio translates into an energy difference of −0.48 kcal/mol (where $\Delta G = -RT \ln K$) in favor of the *trans* isoform. In aqueous solution with no DPC present, the ratio of *trans*/*cis* is 1.46:1 at 288 K based on comparison of the proline δ' to δ'' peaks in a ROESY spectra of **1** (data not shown). With no DPC present, the energy difference between the two isoforms is thus −0.22 kcal/mol. Therefore, binding to DPC stabilizes the *trans* isoform of the peptide by −0.26 kcal/mol.

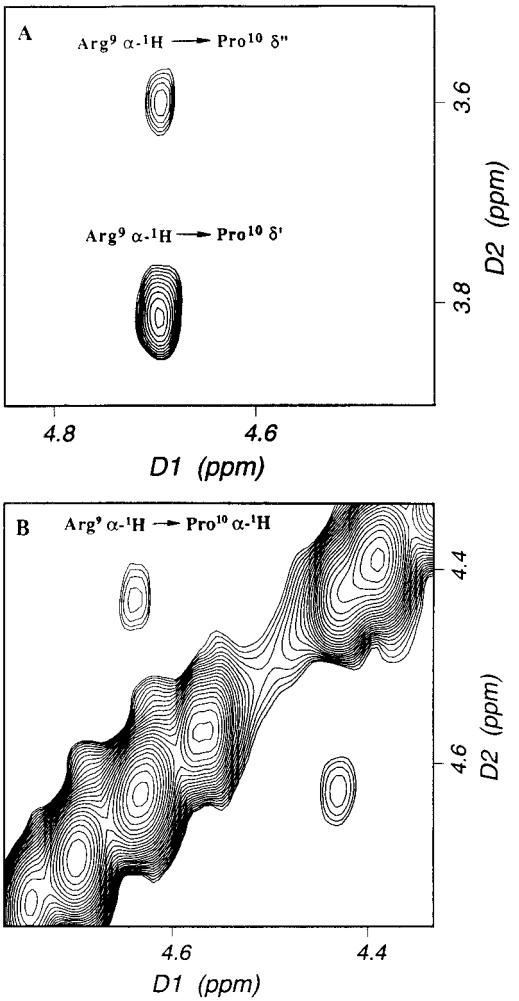

Figure 2. Two expansions of a NOESY spectrum at 500 MHz of **1** with no DPC present showing the Arg^9 α-^{1}H to Pro^{10} δ' to δ'' cross peaks (A) and the Arg^9 α-^{1}H to Pro^{10} α-^{1}H cross peak (B). The spectrum was recorded at 288 K with a mixing time of 200 ms. The sample was 2.18 mM in **1** with 10 mM PO_4^{3-} at pH 3.4 in 100% D_2O.

The finding of the *cis* isoform in **1** was somewhat surprising, since neither dynorphin nor any of its analogs have been shown to exhibit *cis−trans* isomerism about the Arg^9−Pro^{10} ω bond to the best of our knowledge. The *cis−trans* isomerism in the cyclic analog is most likely a result of the cyclization process stabilizing the *cis* isoform in analog **1** relative to that in the native dynorphin. On the basis of the activity profile of **1**, it appears that the active form of the full-length peptide is either the *trans* isoform alone or both isoforms. The rationale for this is that if the active form of dynorphin was the *cis* isoform being represented by a minor unidentified conformation in previous studies, one would expect very high potency for **1** due to its relatively high level of *cis* isoform. However, the peptide exhibits similar potency and selectivity at the κ-opioid receptor as compared to dynorphin.[2] It is also possible that both isoforms are active in the full-length peptide. This could conceivably be true if isomerization of the Arg^9−Pro^{10} ω caused only minor structural changes in the active portions of the peptide. In the case of **1** (*vide infra*), the *cis−trans* isomerism appears to only affect the lipid-mediated structure near the disulfide link. This small structural difference suggests the possibility that both the *cis* and *trans* isoforms are active in analog **1**.

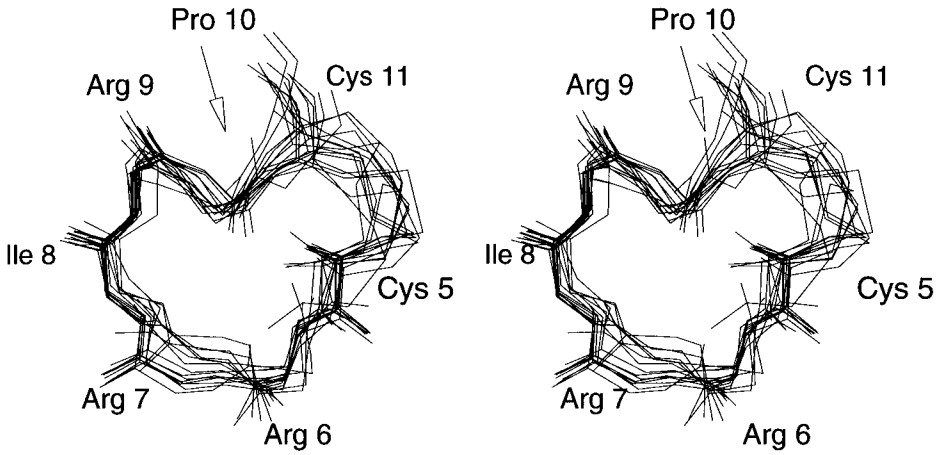

Figure 3. Stereoview of the backbone overlay from residues Cys^5 through Cys^{11} of the 20 final *cis* structures of **1** examined by restrained molecular dynamics (rMD). Each structure in the family represents the averaged trajectory from 60 to 200 ps of the rMD simulations.

Amide Temperature Coefficients. The only amide temperature coefficients below 3.0 ppb/°C of **1** bound to DPC were for the Arg^6 *trans* isoform and the degenerate Arg^7 amide with values of 1.90 and 2.64 ppb/°C, respectively. Since the Arg^7 amide proton chemical shift is degenerate in the *cis* and *trans* isoforms of the peptide, it is impossible to determine *a priori* the values of the Arg^7 coefficient for each respective isoform. In the structures generated for the *cis* isoform of the peptide (*vide infra*), the Arg^7 amide is pointed toward the interior of the ring at the beginning of the β-turn and is not involved in a hydrogen bond. For the *trans* isoform, the Arg^7 amide is pointed away from the interior of the ring in most of the structures examined by rMD. It therefore seems more plausible that the lowered amide temperature coefficient of Arg^7 is due to the position of the amide proton in the *cis* isoform of analog **1**. The low Arg^6 amide temperature coefficient of the *trans* isoform is likely due to the Arg^6 amide being buried in the interior of the peptide. The Arg^6 amide proton is pointed toward the interior of the peptide in the majority of the structures examined by rMD as shown below. Therefore, the Arg^6 amide appears to be solvent shielded and is not part of a hydrogen bond. Lowered amide temperature coefficients have also been observed for leucine enkephalin bound to DPC micelles with no evidence for a hydrogen bond acceptor.[27]

Structural Analysis of the *Cis* Isoform. Analysis of the rMD results for the 20 *cis* structures was initially based on visual inspection with InsightII (Biosym, San Diego). Subsequently the average torsion angles and key distances over the final 140 ps of the 200 ps rMD simulations were examined. The average Arg^7 to Pro^{10} $C_\alpha - C_\alpha$ distance for the 20 structures examined was 4.81 ± 0.51 Å. This $C_{\alpha(i)} - C_{\alpha(i+3)}$ distance of less than 7.0 Å is consistent with the definition of a β-turn.[28] From an analysis of the ϕ and ψ angles of the $i + 1$ and $i + 2$ residues, the structures were classified as type III β-turns.[28] No hydrogen bond was possible across the turn due to the lack of an amide proton on Pro^{10}. The ideal ϕ and ψ values for type III β-turns are −60° and −30° for both the $i + 1$ and $i + 2$ residues, respectively.[28] These ideal values for type III β-turns leads to the classification of 11 of the 20 *cis* structures as ideal type III β-turns, while the remaining nine are classified as nonideal type III β-turns.[28] Nonideal β-turns differ from ideal β-turns such that their ϕ, ψ values have more variability than ideal turns. For the 11 ideal type III β-turns, the average ϕ and ψ angles of the $i + 1$ residue (Ile^8) are −39.9 ± 24.3° and −62.9 ± 9.3°, respectively, and for the $i + 2$ residue (Arg^9) ϕ and ψ are −97.8 ± 8.6° and −43.2 ± 3.4°, respectively. The average ϕ and ψ angles of the $i + 1$ residue (Ile^8) for the nine nonideal type III β-turn structures are −134.2 ± 19.0° and −66.5 ± 7.0°, respectively, and for the $i + 2$ residue (Arg^9) ϕ and ψ are on average −85.4 ± 12.4° and −40.0 ± 4.2°, respectively. These data are summarized in Table 4 (Supporting Information), which contains the average ϕ, ψ angles for residues Ile^8 and Arg^9 for the final 160 ps of the rMD simulations. Examination of these data reveal that the difference in the structural classification is largely due to variability in the Ile^8 ϕ angle. The structural statistics in Table 1 show that the final family of 20 *cis* structures has an average pairwise root mean square deviation of 0.85 ± 0.37 Å for the Cys^5 through Cys^{11} backbone portion of the molecule. Further structural statistics are summarized in Table 1. The NOE violations and target functions are all reasonably low after the DIANA calculations. As expected, the energies remain rather high until van der Waals terms are included and energy minimization is performed; restrained molecular dynamics further lowers the energies. Figure 3 contains a stereoview of the backbone overlay of the ring portion for the final family of 20 *cis* structures.

Structural Analysis of the *Trans* Isoform. As in the case of the *cis* isoform, the 20 rMD simulations of the *trans* isoform were averaged from 60 to 200 ps and the resulting structures examined with InsightII (Biosym, San Diego). The assignment of the secondary structural elements in the *trans* isoform of **1** proved more difficult than in the *cis* case for reasons described below. One of the standard measures for determining β-turns in proteins and peptides is the requirement that the $C_{\alpha(i)} - C_{\alpha(i+3)}$ distance in nonhelical regions be less than 7.0 Å.[28] On the basis of this definition, the averaged rMD structures of the *trans* isoform have a β-turn in the ring portion of the molecule from Cys^5 to Ile^8 with an average $C_{\alpha(i)} - C_{\alpha(i+3)}$ distance of 5.74 ± 0.20 Å. The actual assignment of the Cys^5 to Ile^8 β-turn to a specific type is precluded by inconsistencies in the Arg^6 ϕ and Arg^7 ψ backbone torsion angles. The low preci-

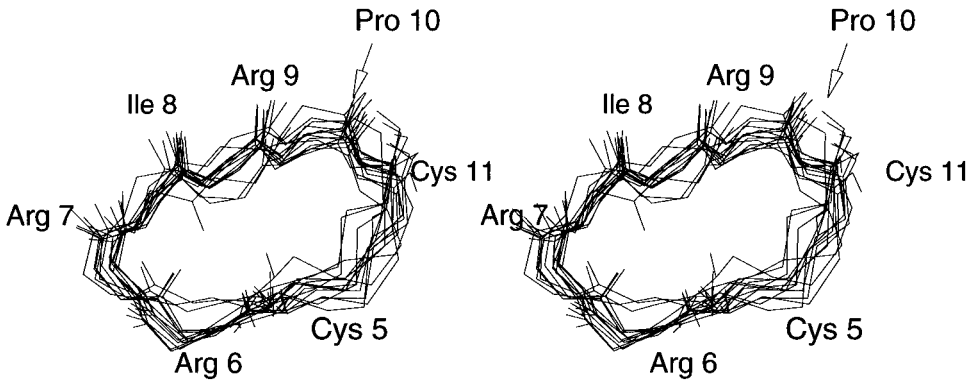

Figure 4. Stereoview of the backbone overlay from residues Cys[5] through Cys[11] of the 20 final *trans* structures of **1** examined by restrained molecular dynamics (rMD). Each structure in the family represents the averaged trajectory from 60 to 200 ps of the rMD simulations.

sion in the Arg[6] ϕ torsion angle is a result of the variability on the position of the Cys[5] carbonyl, which appears to adopt a wide variety of positions. Similarly, the variability in the Arg[7] ψ torsion angle is caused by the Arg[7] carbonyl adopting multiple positions. In contrast, the Arg[6] ψ and Arg[7] ϕ angles are fairly well defined. These data are summarized in Table 5 (Supporting Information), which shows the average ϕ and ψ angles for the Arg[6] and Arg[7] residues of the *trans* isoform of **1**. The structural statistics compiled in Table 1 show that the final family of 20 *trans* structures have an average pairwise root mean square deviation of 0.95 $\pm$ 0.29 Å for the Cys[5] through Cys[11] backbone portion of the molecule. Additional structural statistics for all the calculations are shown in Table 1. The NOE violations and target functions are again all reasonably low after the DIANA calculations. As expected, the energies remain rather high until van der Waals terms are included and energy minimization is performed; restrained molecular dynamics further lowers the energies. Figure 4 is a stereoprojection of the backbone overlay of the final family of 20 *trans* structures examined by rMD.

Comparison of *Cis* and *Trans* Isoforms with Other Dynorphin Models. Neither the *cis* nor *trans* isoforms of **1** exhibited an α-helical NOE pattern, nor did the rMD simulations indicate an α-helical structure in the peptides. The α-helical structure is predicted by Schwyzer and others to be the lipid-mediated active form of dynorphin.[11,12] The differences in structure may be because of how each peptide binds to the DPC micelles. Previous work has shown that the hydrophobic side chains of Phe[4], Leu[5], and Ile[8] in dynorphin all reside on the same face of the α-helix.[15] This arrangement forms an amphipathic α-helix that may be important for interaction with the cell membrane and the receptor. In contrast to the situation in the full-length peptide, analog **1** does not contain the native Leu[5] residue, and the Phe[4] and Ile[8] side chains do not appear to be on the same face of the peptide in the *trans* structures. The *cis* isoform does have the Phe[4] and Ile[8] present on the same side of the ring where they may interact with the lipid micelle in a manner similar to that of the native dynorphin (data not shown). There are also NOEs from the Phe[4] side chain to the Ile[8] side chain in the *cis* isoform, indicating that the two side chains are in similar locations in three-dimensional space.

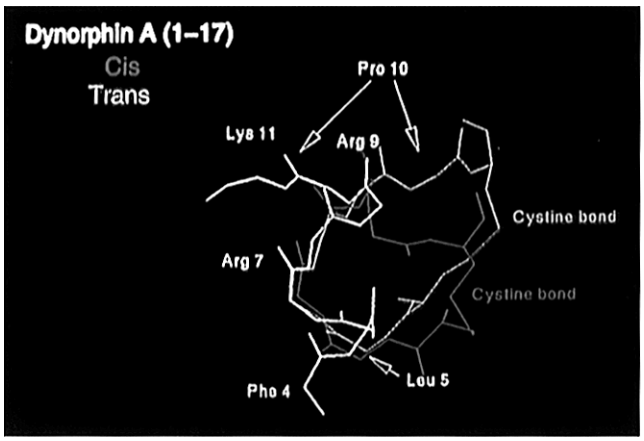

Figure 5. Stereoview of the backbone overlay from residues Arg[6] through Arg[9] of dynorphin A (yellow),[15] a *trans* isoform of **1** (purple), and a *cis* isoform of **1** (red).

It has become increasingly clear that the topographical features (i.e. the three-dimensional arrangement of side chains in space) of peptide hormones are as important for activity as the conformational features of the backbone.[6,29,30] It is quite possible to have a different topography in the case of two compounds with similar secondary structures, or to have similar topographies in compounds which lack the same secondary structural elements.[29] The latter may be operative as the key side chains in the middle of the peptide in both isoforms of **1** and the native dynorphin appear to present similarly, despite their apparent differences in global structure. Figure 5 contains a backbone overlay from residues Arg[6] through Arg[9] of a representative structure of dynorphin, a representative structure of the *trans* isoform of **1**, and a *cis* structure of **1**. The overlay of the three molecules shows similarities in a region of dynorphin that is critical for activity. The key differences in the *cis* and *trans* isoforms of **1** are in the region near the cystine bond in each molecule. This is also where the largest chemical shift differences take place in the two isoforms. When the cyclic dynorphin analog **1** is bound to DPC micelles, the Arg[6], Arg[7], and Ile[8] shifts become degenerate. The backbone positions of these residues, and the ^{1}H shift degeneracy, indicates that they may be in similar chemical environments. The backbone RMSD between the top five *cis* and *trans* rMD structures is 1.11 $\pm$ 0.17 Å for residues Arg[6] through Arg[9]. When residues Cys[5], Pro[10], and Cys[11] are included in the RMSD calculation, the value increases to 2.15 $\pm$

0.22 Å. The RMSD between the top five average *cis* rMD structures and the top five structures from our dynorphin work is 1.04 ± 0.14 Å from Arg^6 through Arg^9. The same calculation for the top five *trans* rMD structures gives a value of 1.38 ± 0.13 Å. This comparison makes it evident that, despite differences in secondary structural elements, there are common threads in the structures of the native dynorphin and the two isoforms of **1** presented here. The similar backbone positions in the different secondary structural elements may be important for placing key peptide side chains into their active positions.

Conclusions

This study represents a part of our effort to determine the structure of opioid peptide hormones in identical, chemically anisotropic environments.[9,14,15,27] The advantages of using DPC micelles to mimic the cell membrane are mediated by the disadvantages inherent in the character of the peptide lipid complexes. These may include increased line width and unfavorable exchange rates. Although the motional characteristics of a peptide-micelle complex approach that of a small protein, there are usually no long-range NOEs. Thus the resolution of the structures suffer as compared to proteins. As the evidence for the involvement of the membrane in opioid peptide activity is increasing, however, micelles provide a reasonable mimic for such interactions.

The results presented herein indicate the possibility that the similar activity of the cyclic dynorphin analog **1**, despite the fact that **1** contains approximately 30% of the *cis* isoform about the Arg^9−Pro^{10} amide bond, and dynorphin is due to the fact that both isoforms of **1** are κ-opioid agonists. The three-dimensional positioning of key side chains in residues Arg^6, Arg^7, Ile^8, and Arg^9 may be of the correct spatial proximity to bring about agonist activity in the *cis* and *trans* isoforms of **1**. The topographical positions of the side chains may be more important in this case than the backbone conformation when comparing the results presented here with previous dynorphin models. Further structure−activity studies on dynorphin analogs locked in either the *cis* or *trans* isoform at the Arg^9−Pro^{10} ω bond would be useful to determine the exact binding conformation of **1** as well as dynorphin.

Acknowledgment. The authors gratefully acknowledge Dr. Vikram Roongta of the Biochemistry/Biomedical Engineering NMR Center at the University of Minnesota, Mr. Paul M. Anderson of the University of Minnesota Supercomputer Institute, and Mr. Charles Watts from the University of Minnesota, Department of Biochemistry, for continued technical support. This work was supported by a grant from the Petroleum Research Fund, administered by the American Chemical Society (D.A.K.), and by NIDA grant DA-04248 (V.J.H.). M.R.T. was supported in part by the Molecular Biophysics Training Program NIH No. 5T32 GM08277-07 and by the University of Minnesota, Department of Medicinal Chemistry.

Supporting Information Available: ^{1}H NMR chemical shift data for compound **1** in water (Table 3), average φ, ψ angles for the $i + 1$ and $i + 2$ residues of the type III β turn in the *cis* (Table 4), and average φ, ψ angles for the $i + 1$ and $i + 2$ residues of β turn in the *trans* (Table 5) (4 pages). Ordering information is given on any current masthead page.

References

(1) Kawasaki, A. M.; Knapp, R. J.; Kramer, T. H.; Wire, W. S.; Vasquez, O. S.; Yamamura, H. I.; Hruby, V. J. Design and Synthesis of Highly Potent and Selective Cyclic Dynorphin A Analogues. *J. Med. Chem.* **1990**, *33*, 1874−1879.

(2) Meyer, J. P.; Collins, N.; Lung, F. D.; Davis, P.; Zalewska, T.; Porrcea, F.; Yamamura, H. I.; Hruby, V. J. Design, Synthesis, and Biological Properties of Highly Potent Cyclic Dynorphin A Analogues. Analogues Cyclized Between Positions 5 and 11. *J. Med. Chem.* **1994**, *37*, 3910−3917.

(3) Turcotte, A.; Lalonde, J. M.; St. Pierre, S.; Lemaire, S. I. Structure-Function Relationships of Ala-containing Analogs. *Int. J. Pept. Protein Res.* **1984**, *23*, 361−367.

(4) Snyder, K. R.; Story, S. C.; Heidt, M. E.; Murray, T. F.; DeLander, G. E.; Aldrich, J. V. Effect of Modulation of the Basic Residues of Dynorphin A (1−13) Amide on Kappa Opioid Receptor Selectivity and Opioid Activity. *J. Med. Chem.* **1992**, *35*, 4330−4333.

(5) Kawasaki, A. M.; Knapp, R. J.; Walton, A.; Wire, W. S.; Zalewska, T.; Yamamura, H. I.; Porrcea, F.; Burks, T. F.; Hruby, V. J. Syntheses, Opioid Binding Affinities, and Potencies of Dynorphin A Analogues Substituted in Positions 1, 6, 7, 8, and 10. *Int. J. Pept. Protein Res.* **1993**, *42*, 411−419.

(6) Hruby, V. J. Conformational Restrictions of Biologically Active Peptides Via Amino Acid Side Chain Groups. *Life Sci.* **1982**, *31*, 189−199.

(7) Kessler, H.; Steurnagel, S. Conformational Determination by NMR Spectroscopy. In *Peptide Pharmaceuticals*; Ward, D., Ed.; Elsevier: New York, 1992; pp 18−46.

(8) Henry, G. D.; Sykes, B. D. Methods to Study Membrane Protein Structure in Solution. *Methods Enzymol.* **1994**, *239*, 515−535.

(9) Kallick, D. A.; Tessmer, M. R.; Watts, C. R.; Li, C.-Y. The Use of Dodecylphosphocholine Micelles in Solution NMR. *J. Magn. Reson., Ser. B* **1995**, *109*, 60−65.

(10) Moroder, L.; Romano, R.; Guba, W.; Mierke, D. F.; Kessler, H.; Delporte, C.; Winand, J.; Christophe, J. New Evidence for a Membrane-Bound Pathway in Hormone Receptor Binding. *Biochemistry* **1993**, *32*, 13551−13559.

(11) Erne, D.; Sargent, D. F.; Schwyzer, R. Preferred Conformation, Orientation, and Accumulation of Dynorphin A-(1−13)-tridecapeptide on the Surface of Neutral Lipid Membranes. *Biochemistry* **1985**, *24*, 4261−4263.

(12) Schwyzer, R. In Search of the 'Bio-active Conformation'- Is it Induced by the Target Cell Membrane? *J. Mol. Recognit.* **1995**, *8*, 3−8.

(13) Collins, N.; Hruby, V. J. Prediction of the Conformational Requirements for Binding to the κ-Opioid Receptor and Its Subtypes. I. Novel α-Helical Cyclic Peptides and Their Role in Receptor Selectivity. *Biopolymers* **1994**, *34*, 1231−1241.

(14) Kallick, D. A. Conformation of Dynorphin A(1−17) Bound to Dodecylphosphocholine Micelles. *J. Am. Chem. Soc.* **1993**, *115*, 9317−9318.

(15) Tessmer, M. R.; Kallick, D. A. *Biochemistry* **1997**, *36*, 1971−1981.

(16) Wüthrich, K. *NMR of Proteins and Nucleic Acids*; Wiley: New York, 1986.

(17) Marion, D.; Wüthrich, K. Application of Phase Sensitive Two-Dimensional Correlated Spectroscopy (COSY) for Measurements of ^{1}H-^{1}H Spin-Spin Coupling Constants in Proteins. *Biochem. Biophys. Res. Commun.* **1983**, *113*, 967−974.

(18) Macura, S.; Ernst, R. R. Elucidation of Cross Relaxation in Liquids by Two-Dimensional NMR Spectroscopy. *Mol. Phys.* **1980**, *41*, 95−117.

(19) Olejniczak, E. T.; Eaton, H. L. Extrapolation of Time-Domain Data with Linear Prediction Increases Resolution and Sensitivity. *J. Magn. Reson.* **1990**, *87*, 628−632.

(20) Bothner-By, A. A.; Stephens, R. L.; Lee, J.-M.; Warren, C. D.; Jeanloz, R. W. Structure Determination of a Tetrasaccharide: Transient Nuclear Overhauser Effects in the Rotating Frame. *J. Am. Chem. Soc.* **1986**, *106*, 811−813.

(21) Bax, A.; Davis, D. G. Practical Aspects of Two-Dimensional Transverse NOE Spectroscopy. *J. Magn. Reson.* **1985**, *63*, 207−213.

(22) Amodeo, P.; Castiglione, A. C.; Motta, A. Multiple Conformations and Proline *cis-trans* Isomerization in Salmon Calcitonin: A combined Nuclear Magnetic Resonance, Distance Geometry, and Molecular Mechanics Study. *Biochemistry* **1994**, *33*, 10754−10762.

(23) Güntert, P.; Braun, W.; Wüthrich, K. Efficient Computation of Three-Dimensional Protein Structures in Solution from Nuclear Magnetic Resonance Data Using the Program DIANA and the Supporting Programs CALIBA, HABAS, and GLOMSA. *J. Mol. Biol.* **1991**, *217*, 517−530.

(24) Güntert, P. *DIANA User's Manual and Instructions*, version 2.1; Institut für Molekularbiologie und Biophysik Eidgenössiche Technische Hochschule-Hönggerberg: Zürich, 1993.

(25) Williamson, M. P.; Havel, T. F.; Wüthrich, K. Solution Conformation of Proteinase Inhibitor IIA from Bull Seminal Plasma by ^{1}H Nuclear Magnetic Resonance and Distance Geometry. *J. Mol. Biol.* **1985**, *182*, 295−315.
(26) Weiner, S. J.; Kollman, P. A.; Nguyen, D. T.; Case, D. A. An All Atom Force Field for Simulations of Proteins and Nucleic Acids. *J. Comput. Chem.* **1986**, *7*, 230−252.
(27) Watts, C. R.; Tessmer, M. R.; Kallick, D. A. Structure of Leu^5-Enkephalin Bound to a Model Membrane as Determined by High-Resolution NMR. *Lett. Pept. Sci.* **1995**, *2*, 59−70.
(28) Ball, J. B.; Hughes, R. A.; Alewood, P. F.; Andrews, P. R. β-Turn Topography. *Tetrahedron* **1993**, *49*, 3467−3478.
(29) Hruby, V. J.; Al-Obeidi, F.; Kazmierski, W. Emerging Approaches in the Molecular Design of Receptor-Selective Peptide Ligands: Conformational, Topographical, and Dynamic Considerations. *Biochem. J.* **1990**, *268*, 249−262.
(30) Hruby, V. J. Conformational and Topographical Considerations in the Design of Biologically Active Peptides. *Biopolymers* **1993**, *33*, 1073.

JM960562M